Metallurgical and Materials Engineering
Association of Metallurgical Engineers of Serbia AMES

Scientific paper
UDC: 661.66
66.018.9:661.66

INTRODUCTION OF NANO-LAMINATE TI_3SiC_2 AND SiC PHASES INTO C_f-C COMPOSITE BY LIQUID SILICON INFILTRATION METHOD

Omid Yaghobizadeh[1]*, *Arman Sedghi*[1], *Hamid Reza Baharvandi*[2]

[1] *Department of Materials Engineering, Imam Khomeini International University, Qazvin, Iran*
[2] *Department of Materials Science and Engineering, MUT, Tehran, Iran*

Received 10.02.2017
Accepted 10.03.2017

Abstract

The material C_f-C-SiC-Ti_3SiC_2 is promising for high temperature application. Due to the laminated structure and special properties, the Ti_3SiC_2 is one of the best reinforcements for C_f-C-SiC composites. In this paper, C_f-C-SiC-Ti_3SiC_2 composites were fabricated by liquid silicon infiltration (LSI) method; the effect of the TiC amount on the various composites properties were studied. For samples with 0, 50 and 90 vol.% of TiC, the results show that bending strength are 168, 190, and 181 MPa; porosities are 3.2, 4.7, and 9%; the fracture toughness are 6.1, 8.9, and 7.8 $MPa{\cdot}m^{1/2}$; interlaminar shear strength are 27, 36, and 30 MPa; the amount of the MAX phase are 0, 8.5, and 5.6 vol.%, respectively. These results show that amount of TiC is not the main effective parameter in synthesis of Ti_3SiC_2. The existence of carbon promotes the synthesis of Ti_3SiC_2 indicating that only sufficient carbon content can lead to the appearance of Ti_3SiC_2 in the LSI process.

Keywords: *Ti_3SiC_2; SiC; LSI; Ceramic matrix composite.*

Introduction

In recent years, carbon composites have attracted many attentions because of their low density, thermal shock resistance, high fracture toughness and excellent mechanical strength at high temperatures [1]. Silicon layer can protect composites against ablation environments in temperatures even higher than 1700 °C [2], but this layer cannot resist very high temperatures and flow of high pressure gasses. In few previous decades, the addition of the super-high temperature ceramics to the matrix have provided good resistance of composites against ablation environments [3-6]. The

---

* Corresponding author: Omid Yaghobizadeh, *omid_yaghobi@yahoo.com*

MAX Ti_3SiC_2 phase has been interesting to researchers because of its nanolaminate layer structure and excellent properties [7]. The Ti_3SiC_2 can sustain various micro-deformation to deflect the cracks. Therefore, it is expected that the addition of MAX phase into the matrix can increase bending strength and other mechanical properties. Melting temperature of the refractory Ti_3SiC_2 phase is higher than 3000 °C [8]. Induction of this phase into the matrix can provide better resistance against ablation due to its refractory properties [9].

Usually, Cf–C–SiC–Ti_3SiC_2 composites are fabricated by several methods: (a) polymer impregnation and pyrolysis (PIP), (b) using Ti_3SiC_2 as the inert filler, (c) by joint process of PIP and liquid silicon infiltration (LSI), (d) by joint process of slurry infiltration and LSI, and also (e) by LSI method [1]. In this paper, Ti_3SiC_2 and SiC were introduced into Cf–C composites by LSI method and effect of volume ratio of TiC *vs*. phenolic resin on the microstructure, bending strength, fracture toughness, interlaminar shear strength and amount of Ti_3SiC_2 were investigated.

Materials and methods

Composites fabrication contains many steps, as illustrated in Fig 1. The primary step is the manufacture of carbon fiber preform (carbon and TiC in the matrix). The high purity TiC powder used in this test has an average particle size of 3 to 5 μm, surface area of 2.2 m^2/g and 0.11% of remaining carbon. In this study, TiC powder was mixed with the different proportions of phenolic resin (0:100, 50:50 and 90:10). This mixture was embedded between the layers of carbon fiber (1K, T-300), and then after warm pressing it was pyrolyzed at 1000 °C for 1h to convert the resin to carbon and form open pores in the structure. In the second step the preforms were infiltrated together with liquid silicon at 1500 °C.

The infiltration process was performed in vacuumed graphite furnace at heating rate of 10 °C/min. After the infiltration process, the temperature was reduced to 1350 °C and samples were kept at this temperature for 1.5 h. The purpose of this process was to form Ti_3SiC_2 by solid state reactions. The bending strength was carried out through the three-point bending method, according to ASTM C-1341 standard. Eleven samples were tested to obtain an average strength. The loading rate was 0.5 mm/min and the support span was 30 mm. The fracture toughness, was measured using single edge notched beam method under three-point bending test with a loading speed of 0.05 mm/min. The support span was 30 mm and twelve samples were tested to obtain an average fracture toughness. The interlaminar shear strength was performed with the double-notched compressive method, according to ASTM C1292-00 standard. The porosity percentage of the specimens was measured by Archimedes method according to ASTM C-20 standard. X-ray diffraction (XRD, GNR, and MPD 3000) analysis was employed to investigate the composition of obtained ceramics. Microstructural characterizations of samples were investigated by scanning electron microscopy (SEM TESCAN), applying back-scattered electron image (BSE) and energy dispersive spectroscopy (EDS).

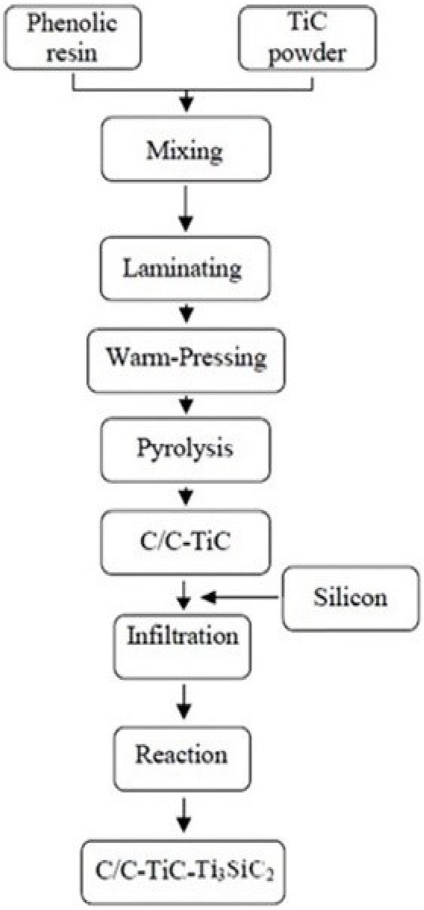

Fig. 1. Steps manufacture of C_f-C-SiC-Ti_3SiC_2 composite

Results and discussion

Porosity of the preforms and liquid silicon infiltration (LSI)

The powders were ground in disc mill in order to enhance the activation of TiC particles and inhibit agglomeration due to fine-sized particles. Physical properties of the samles with different volume proportion of TiC resin were compared in Table 1. The porosity of the preforms increased from 21.3 % to 36.3% for the sample without and with 90 vol.% of TiC, respectively. The corresponding density increased with increasing amount of TiC particles from 1.3 to 1.8 g/cm³.

Table. 1. Properties of the samples A, B and C

Sample	A	B	C
TiC phenolic resin [vol.%]	0:100	50:50	90:10
Open porosity [%] (Preform)	21.3	27.9	36.3
Bulk density[g/cm^3](Preform)	1.3	1.6	1.8
Open porosity[%] (Final composites)	3.2	4.7	9
Bending strength [MPa]	168±20	190±31	181±26
Fracture toughness [MPa.m$^{1/2}$]	6.1±1	8.9±1.2	7.8±1.4
Interlaminar shear strength [MPa]	27±4	36±6	30±4

At 1500 °C, the molten silicon infiltrates into the porous preform due to its capillary force. The amount of capillary force evidently depends on the structure of pores and can be calculated as follows:

$$\Delta P = \left(\frac{S_p}{V_p}\right) \cdot \gamma_{LV} \cos\theta \tag{1}$$

where: γ_{LV} is the liquid/vapor interfacial energy, V_P is the pore volume, θ is the wetting angle, and S_P is the pore surface area. Infiltration time (t) can be determined by the following formula:

$$t = \frac{h^2\eta}{-2K_0\Delta P} \tag{2}$$

where: K_0 is a permeability constant, h is the infiltration depth, and η is the fluid viscosity. When the TiC particles are embedded between the carbon fabrics, the inter-bundle pores of matrix change to a high number of inter-particle pores. Thus, according to Eq. (1) the volume of pores will be reduced and the surface of pores will increase. As a result, the enhancement of *Sp/Vp* proportion will increase the capillary force.

The TiC particles and carbon have appropriate wettability with molten silicon at 1500 °C [10, 11]. According to *L.R. Katipelli et al.* [10], *H. Sasaki et al.* [12] and *H. Nakanishi et al.* [13], the wetting angle between silicon melt and the particles, the viscosity of silicon melt, and the surface tension of silicon melt are: 32°, 0.8 mPa·s, and 0.740 J/m2, respectively. The pore volume fraction of the preforms was increased from 27.9% to 36.3%, for the sample with 50 vol.% TiC and 90 vol.%; the particle shape factor is 1 [14].

Therefore, for the present preform, 1.4 s and 2.08 s are the approximated infiltration time, indicating that the molten silicon can penetrate rapidly into the preform.

Phase analysis and thermodynamic analysis

XRD patterns of the final composites are shown in Fig. 2. As it can be seen, sample A is composed of SiC and silicon, samples B and C are composed of SiC–$TiSi_2$–Ti_3SiC_2–silicon and small amount of TiC. During the LSI process, molten silicon, TiC particles and carbon react, leading to the formation of Ti-Si-C matrix.

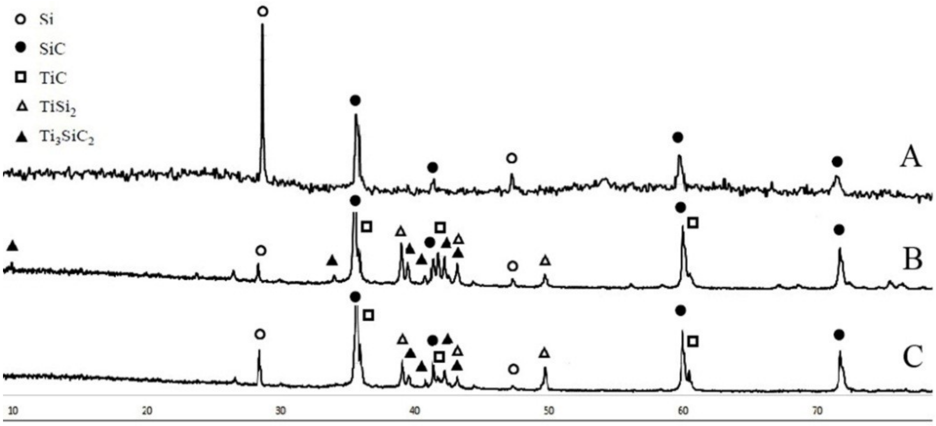

Fig. 2. XRD patterns of samples A, B and C after infiltration.

The polished-surface morphologies of samples A and B are shown in Fig. 3. Gray area is a region of SiC phase in the matrix, and the bright area is associated with unreacted Si, as it was confirmed with EDS analysis (Fig. 4).

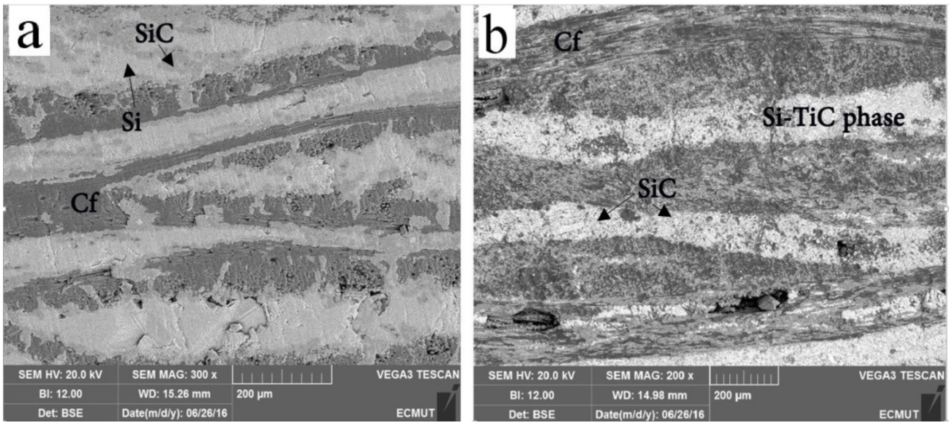

Fig. 3. BSE images of the polished-surface of composite A (a), and composite B (b).

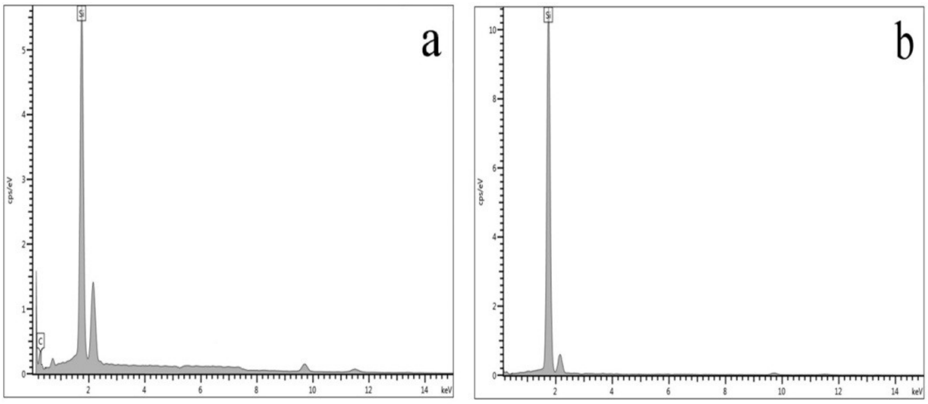

Fig. 4. EDS analysis of grey (a), and bright (b) areas in the Fig. 3a.

The matrix of composite B can be clearly seen in the high magnification of BSE image (Fig. 5), where the bright white area, grey area, and grey bright area are composed of Ti_3SiC_2 phase, SiC phase and $TiSi_2$ phase, respectively. This result was confirmed by EDS analysis (Fig. 5 *b,c,* and *d*).

In sample A, B, and C, the formation of SiC phase can be favored according to the equation:

$$Si(l) + C \rightarrow SiC \qquad \Delta G = -56.9\ kJ/mol \qquad (3)$$

In sample B and C, TiC may react with silicon according to the following reaction:

$$3TiC(s) + 2Si(l) = Ti_3SiC_2(s) + SiC(s) \qquad \Delta G = -75.0\ kJ/mol \qquad (4)$$

The TiC may also react with silicon and carbon, forming Ti_3SiC_2 [8]:

$$9TiC(s) + 8Si(l) + 2C(s) = 3Ti_3SiC_2(s) + 5SiC(s) \qquad \Delta G = -338.7 kJ/mol \qquad (5)$$

According to the thermodynamic calculations it is highly probable that in the presence of carbon (Eq. (5)) formation of Ti_3SiC_2 is more favorable than in the absence of this element (Eq. (4)).

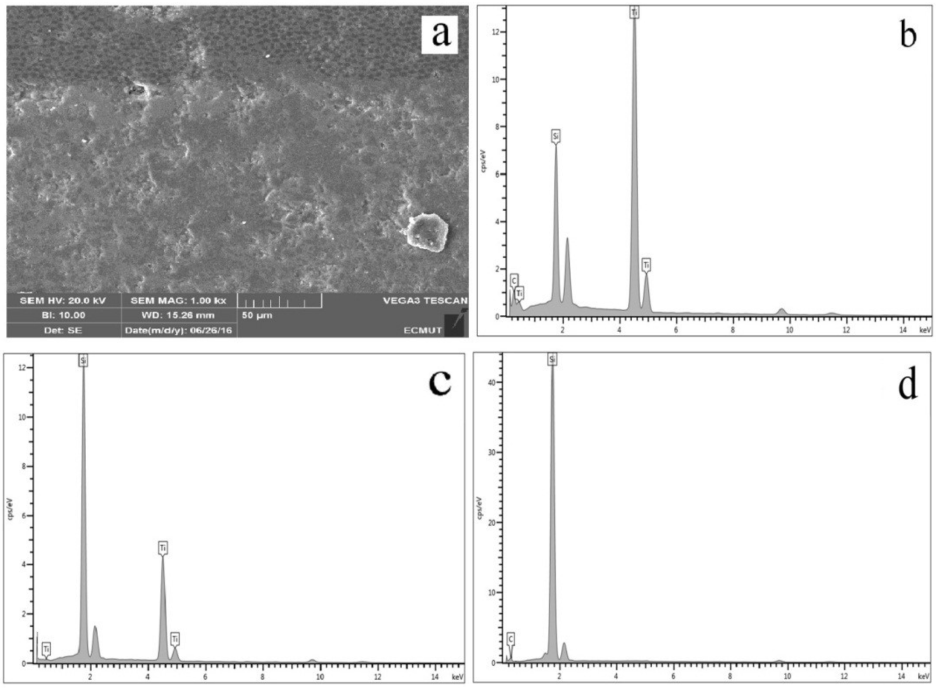

Fig. 5. High magnification image of matrix in the fig. 3b (a), and EDS spectrum of bright white (b), grey bright (c) and grey (d) areas.

The Ti_3SiC_2 content in the samples B and C was 8.5 and 5.6 vol.%, respectively, which was estimated by the Rietveld method.

It was expected that the Ti_3SiC_2 content increases with increasing amount of the TiC particles in the preform, but the results show opposite: the amount of the MAX phase decreases with increasing amount of TiC particles. At position of 10° 2Theta, Ti_3SiC_2 peak was not detectable for the sample C, appears in the sample B with 50 vol.% of TiC in the preform. For sample C intensity of the first peak for the Ti_3SiC_2 decreases.

These results show that amount of TiC is not the main effective parameter in synthesis of Ti_3SiC_2 exclusively, but this reaction is promoted at the presence of sufficient carbon for each mole of TiC (TiC/C molar ratio equal to 4.5) according to Eq. (5). Carbon yield, for used phenolic resin, is about 60%. Therefore, TiC/C molar ratio for the sample B and C is about 2 (or less) and 14.4 respectively.

Mechanical properties of samples

For samples A, B, and C, the bending strength of the composites are: 168, 190, and 181 MPa, respectively (Table 1). Bending strength for the samples B and C are improved in comparison to sample A, due to the replacement of Si by the in situ formed MAX phase. Also, the cracks propagate and cause the delamination of Ti_3SiC_2 layers in the structure due to the lower bonding energy of Ti-Si bonds in comparison to the Ti-C bonds [15].

The Ti_3SiC_2 phase represents a series of deformation modes such as: delamination, kinking, buckling and bending due to its special atomic bonding and lamellar structure, causing fracture energy absorption. In this study, the deformation mechanism contains kink band, fracture of grains, delamination of lamellae of Ti_3SiC_2 and intergranular cracking under different loading modes which are illustrated in Fig. 6. Therefore, the Ti_3SiC_2 induction improves resistance to crack propagation in the matrix.

The induction of Ti_3SiC_2 into the matrix is beneficial for improving the resistance to crack propagation, thereby inhibiting the crack propagation in the matrix. Among all samples, sample B shows the highest toughness, whereas sample A shows the lowest one.

The presence of small pores can increase samples toughness by blinding crack tips in the matrix, while the cracks will spread easily through a dense matrix [16]. On another hand, according to mentioned characteristics of Ti_3SiC_2, the induction of this phase into a dense matrix can cause higher toughness. Thus, the absence of the MAX phase and low porosity of sample A cause low toughness. On the contrary, the greater amount of the MAX phase in sample B will improve toughness.

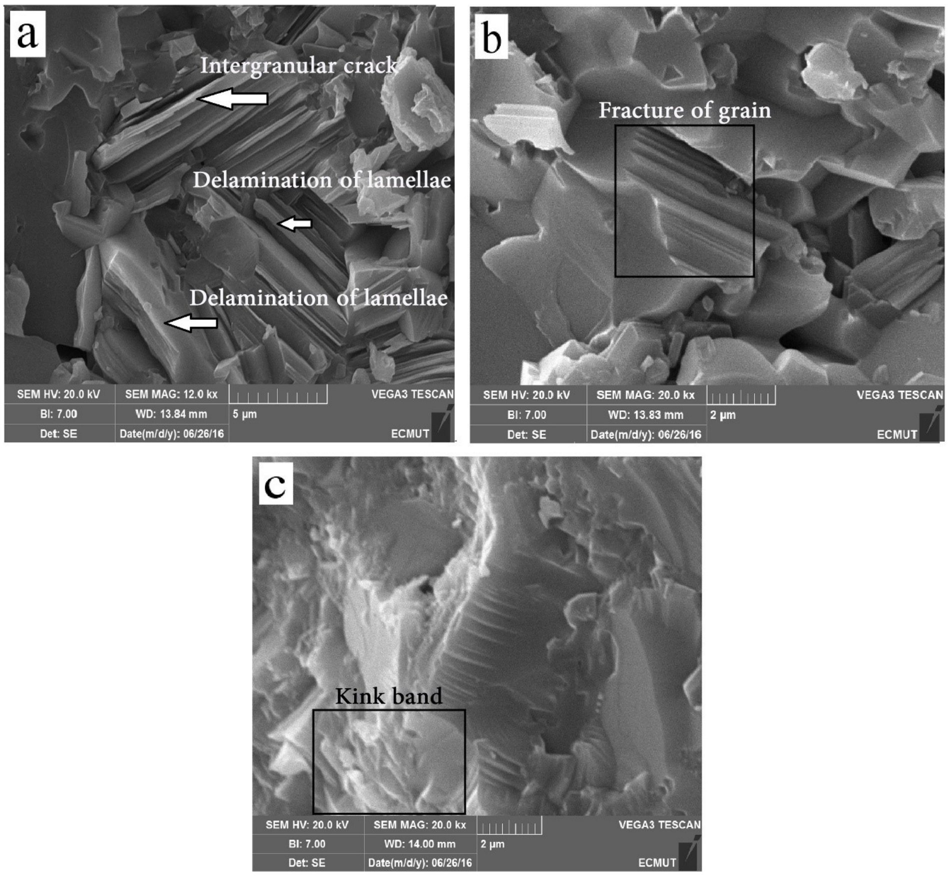

Fig. 6. High magnification of layered morphology of Ti_3SiC_2, the intergranular cracking and delamination of lamellae of Ti_3SiC_2 (a), fracture of grain (b) and kinking band (c).

Fracture surfaces of C_f–C–SiC–Ti_3SiC_2 composite (Sample B) and C_f–C–SiC composite (Sample A) are illustrated in Fig. 7. It is obvious from the fracture surface of the samples, that fiber pullout happened in the sample A, which proves low strength of the matrix and poor bonding between the matrix and the fibers.

It is clear from Fig. 7b that carbon fibers are torn in the sample B, which can be attributed to the high strength of the matrix and high bonding strength between the matrix and fibers. The net result of all these factors is better bending strength. The pulled-out fibers are not short in the C_f–C–SiC composite, and it may be concluded that the fibers have a considerable effect on the composite strength.

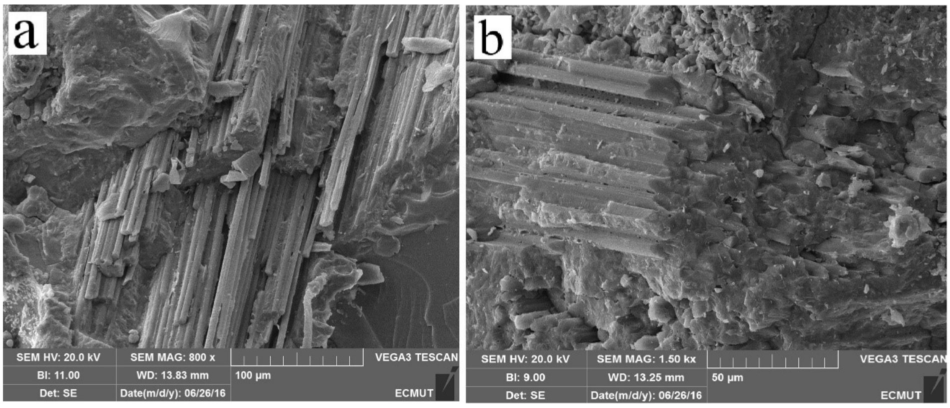

Fig. 7. Fracture-surface morphologies of composite A and B showing the pulled out fibers (a) and sheared fibers (b), respectively.

As shown in Table 1, the interlaminar shear strengths of samples A, B, and C are 27±4, 36±6 and 30±4 MPa. The interlaminar shear strength of all composites were simply depended on the strength of the fibers/matrix connection [16]. The differences between the amounts of interlaminar shear strength of the samples can depend on this parameter. Thus, it can be stated that the bond strength of fibers/matrix of the sample B is higher than of other samples.

According to the mentioned mechanisms and mechanical properties of the samples, it can be proved that the presence of the MAX phase can cause improvement in C_f–C–SiC composites properties.

Conclusion

In summary, C_f–C–SiC–Ti_3SiC_2 and C_f-C-SiC composites were fabricated by the LSI method at 1500°C. The amounts of the MAX phase were 0, 8.5, and 5.6 vol.% for the samples with 0, 50, and 90 vol.% of the TiC, respectively. The results show that the volume percentage of Ti_3SiC_2 phase decreases with increasing the TiC/C molar ratio, and mechanical properties of the samples increase with introduction of Ti_3SiC_2 phases in the C_f–C–SiC composite. The deformation mechanisms in the Ti_3SiC_2 involve kink band, fracture of grains, delamination of lamellae and intergranular cracking.

References

[1] X. Fan, X. Yin, L. Wang, L. Cheng, L. Zhang: Corros. Sci, 74 (2013) 98-105.
[2] M.J.H. Balat: J. Eur. Ceram. Soc, 16 (1996) 55–62
[3] Z.Q. Li, H.J. Li, S.Y. Zhang, J. Wang, W. Li, F.J. Sun: Corros. Sci, (2012). 12–19.
[4] S.F. Tang, J.Y. Deng, S.J. Wang, W.C. Liu: Corros. Sci, 51 (2009) 54–61.
[5] Y.G. Wang, W. Liu, L.F. Cheng, L.T. Zhang: Mater. Sci. Eng. A, 524 (2009) 129–133.
[6] Y. Wang, Y.D. Xu, Y.G. Wang, L.F. Cheng, L.T. Zhang: Mater. Lett, 64 (2010) 2068–2071.
[7] H. Foratirad, HR. Baharvandi, M. Ghanadi Maragheh: Mater. Lett, 180 (2016) 219-222.
[8] X. Yina, S. Hea, L. Zhanga, S. Fana, L. Chenga, G. Tianb, T. Li: Mater. Sci. Eng. A. 527 (2010) 835–841.
[9] X. Fan, X. Yin: Adv. Eng. Mater, 16 (2014) 670–683.
[10] L.R. Katipelli, A. Agarwal, N.B. Dahotre: Appl. Surf. Sci, 153 (2000) 65–78.
[11] K. Mlungwane, I. Sigalas, M. Herrmann, M. Rodriguez: Ceram. Int, 35 (2009) 2435–2441.
[12] H. Sasaki, E. Tokizaki, X.M. Huang, K. Terashima, S. Kimura: Jpn. J. Appl. Phys, 34 (1995) 3432–3436.
[13] H. Nakanishi, K. Nakazato, K. Terashima: Jpn. J. Appl. Phys, 39 (2000) 6487–6492.
[14] J. Lapin, D. Tiberghien, F. Delannay: Intermetallics, 8 (2000) 1429–1438.
[15] X. Fan, X. Yin, X. Cao, L. Chen, L. Cheng, L. Zhang: Compos, Sci Technol.115 (2015) 21–27.
[16] CY. Zhang, HL. Wang, YS. Liu, SR. Qiao, M. Li, D. Han: Vacuum, 105 (2014) 63–68.